Analytical Methods

PAPER

View Article Online
View Journal | View Issue

Cite this: *Anal. Methods*, 2014, **6**, 7343

Design and synthesis of a chemosensor for the detection of Al^{3+} based on ESIPT†

Jing-can Qin, Zheng-yin Yang,* Long Fan, Xiao-ying Cheng, Tian-rong Li and Bao-dui Wang

Received 5th June 2014
Accepted 9th July 2014

DOI: 10.1039/c4ay01330a

www.rsc.org/methods

In this study, a simple fluorescent sensor 2-hydroxybenzcarbaldehyde-(2-methylquinoline-4-formyl) hydrazone (HL) has been designed, synthesized and characterized by ^{1}H-NMR, IR, ESI-MS. Upon addition of Al^{3+}, HL shows a large fluorescence enhancement (220-fold) at 484 nm. The reasons for this phenomenon are attributed to formation of a 1 : 1 complex ($K_a = 5.6 \times 10^4$), which inhibits the excited-state intramolecular proton transfer (ESIPT) process and photo-induced electron transfer (PET) process. Other metal ions including Ba^{2+}, Ca^{2+}, Cd^{2+}, Co^{2+}, Cr^{3+}, Hg^{2+}, K^+, Mg^{2+}, Mn^{2+}, Na^+, Ni^{2+}, Pb^{2+} and Zn^{2+}, have almost no influence on the fluorescence. The lowest detection limit for Al^{3+} is calculated to be 7.2×10^{-7} M in ethanol.

1. Introduction

Aluminium, the most abundant metal on earth, is found in natural waters and most biological tissues in its ionic form, Al^{3+}. As a potential toxic ion, high concentrations of Al^{3+} can hamper plant growth, kill fish and other species in aquatic ecosystems. In addition, it is a non-essential element for biological processes that has been implicated in various neurodegenerative and neurological disorders, such as Alzheimer's disease,[1–5] dialysis encephalopathy, and problems in bone, muscles and so on. According to a WHO report, the average daily human intake of aluminium is approximately 3–10 mg. The tolerable weekly aluminium intake in the human body is estimated to be 7 mg kg^{-1} of body weight.[6] Thus, the detection of Al^{3+} is important to control the concentration levels in the biosphere and minimize direct effects on human health.[7]

In recent years, among several methods[8–10] for the determination of Al^{3+}, the fluorescence method has a wide range of applications because of its operational simplicity, high sensitivity, rapidity, direct visual perception and inexpensive operational cost in medicinal and environmental research. However, compared with other metal cations, the detection of Al^{3+} has always been problematic because of its poor coordination ability, strong hydration ability and the lack of spectroscopic characteristics.[11] Until recently, only a few fluorescent chemosensors had been developed.[12–15] Therefore, the design and synthesis of Al^{3+} selective fluorescent probes have attracted considerable attention.[16,17]

Nitrogen and oxygen-rich coordination environments can provide a hard base environment for the hard acid Al^{3+}. Moreover, the nitrogen and oxygen donor sites can contribute to the high stability of the resultant complexes.[18] Apart from this, the excited-state intramolecular proton transfer (ESIPT) process commonly involves the transfer of an hydroxyl (or amino) proton to an adjacent carbonyl oxygen (or imine nitrogen) through a five- or six-membered ring of hydrogen-bonding configuration. *o*-Hydroxybenzaldehyde, a Schiff base, happens to provide –O–H···N or O···H–N type hydrogen bonds which are a prerequisite for the ESIPT process.[19,20] Taking this in to account, we have designed a Schiff-base ligand which was synthesized by condensing 2-methyl-quinoline-4-carboxylic acid hydrazide with salicylic aldehyde (Scheme 1). Upon binding of Al^{3+}, 2-hydroxybenzcarbaldehyde-(2-methylquinoline-4-formyl) hydrazone (HL) shows a large fluorescence enhancement with turn-on of over 100-fold at 484 nm, which is attributed to the formation of a 1 : 1 stoichiometric complex in ethanol which effects inhibition of an ESIPT process and a photo-induced electron transfer (PET) process.

2. Experimental

2.1. General information

All the chemicals used were obtained from commercial suppliers and used without further purification. ^{1}H-NMR spectra were measured on a Jeol JNM-ECS400 instrument using tetramethylsilane as an internal standard. Electrospray ionization-mass spectroscopy (ESI-MS) were determined on a Bruker Esquire 6000 spectrometer. UV-Vis absorption spectra were recorded on a PerkinElmer Lambda 35 UV-Vis spectrophotometer. Fluorescence spectra were generated on a Shimadzu RF-5301 spectrophotometer equipped with quartz cuvettes with a 1

College of Chemistry and Chemical Engineering, State Key Laboratory of Applied Organic Chemistry, Lanzhou University, Lanzhou 730000, P.R. China. E-mail: yangzy@lzu.edu.cn; Fax: +86 931 8912582; Tel: +86 931 8913515

† Electronic supplementary information (ESI) available. See DOI: 10.1039/c4ay01330a

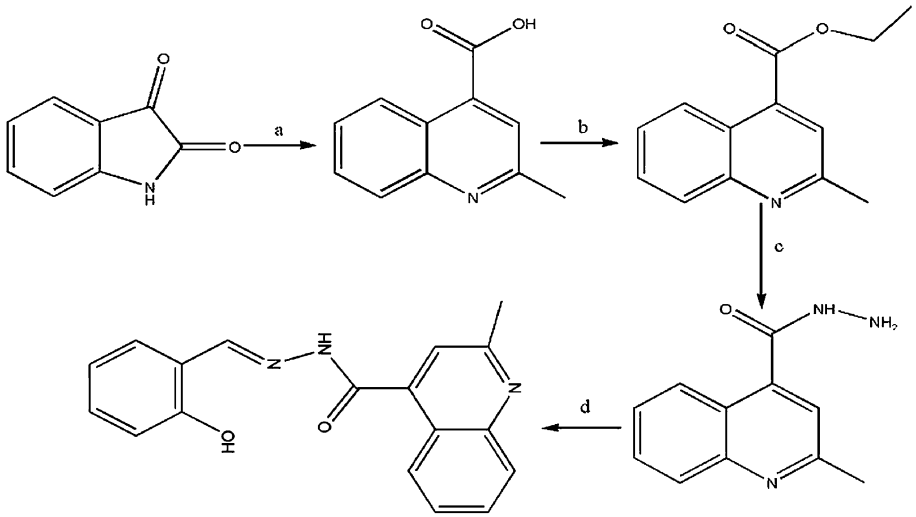

Scheme 1 Reagents and conditions: (a) (i) acetone, aq. KOH, reflux, 15 h; (ii) conc. HCl; (b) conc. H_2SO_4, EtOH, reflux, 18 h; (c) EtOH, $N_2H_4 \cdot H_2O$, 80 °C, 20 h; (d) EtOH, reflux, 10–12 h.

cm path length. The melting point of the Schiff base was determined on a Beijing XT4-100X microscopic melting point apparatus.

2.2. Synthesis

2.2.1. Synthesis of ethyl 2-methyl quinoline-4-carboxylate.[21] A mixture of isatin (6.8 mmol, 1.0 g) and 85% aqueous potassium hydroxide (2.67 g, 47.6 mmol) was heated to 50 °C for 1–1.5 h. Acetone (5 mL, 56.7 mmol) was then added dropwise, maintaining the temperature at 50 °C. After 20 h, the reaction mixture was cooled to room temperature and acidified to pH 3 by addition of concentrated HCl to obtain a heavy slurry which was then filtered, washed, and dried to give a white solid with a melting point (mp) of 248–250 °C. The white solid was used for the next step without further purification. To a solution of 2-methyl quinoline-4-carboxylic acid (3 mmol, 0.56 g) in 75 mL of EtOH was added 3.5 mL of H_2SO_4 (conc.). The resulting reaction mixture was refluxed for 24 h. Solvent was then removed under reduced pressure, and the residue was partitioned between EtOAc and saturated $NaHCO_3$ solution. The organic layer was washed with water and brine, dried over anhydrous Na_2SO_4, filtered, and condensed to give ethyl 2-methyl quinoline-4-carboxylate. Mp: 71–72 °C ^{1}H-NMR (Fig. S1†): (400 MHz, deuterated chloroform ($CDCl_3$)) $\delta = 1.47$ (t, $J = 7.2$ Hz, 3H), 2.82 (s, 3H), 4.51 (q, $J_1 = 7.2$ Hz, $J_2 = 14.0$ Hz, 2H), 7.61 (t, $J = 8.0$ Hz, 1H), 7.76 (t, $J = 8.0$ Hz, 1H), 7.82 (s, 1H), 8.10 (d, $J = 8.4$ Hz, 1H), 8.69 (d, $J = 8.4$ Hz, 1H).

2.2.2. Synthesis of 2-methyl quinoline-4-carboxylic hydrazide. Hydrazine hydrate (80%, 4 mL) was added dropwise to an ethanolic solution (40 mL) of ethyl 2-methyl quinoline-4-carboxylate (5 mmol, 1.015 g). The reaction mixture was refluxed under stirring for 12 h. Then the solvent was concentrated under reduced pressure and let stand overnight in refrigerator. A white needle-like crystal was observed. The final product was filtered, dried and recrystallized from ethanol. Yield: 55%; mp: 178–179 °C. ^{1}H-NMR (Fig. S2†): (400 MHz; CDCl3) $\delta = 2.71$ (s, $3H_e$), 4.25 (s, $2H_h$), 7.29 (s, $1H_f$), 7.54 (m, $1H_b$), 7.59 (s, $1H_g$), 7.73 (m, $1H_c$), 8.05 (d, $J = 8.4$ Hz, $1H_d$), 8.14 (d, $J = 8.1$ Hz, $1H_a$).

2.2.3. Synthesis of 2-hydroxybenzcarbaldehyde-(2-methyl-quinoline-4-formyl) hydrazone (HL). An ethanolic solution (20 mL) of 2-methyl quinoline-4-carboxylic hydrazide (1 mmol, 0.203 g) was added to another ethanolic solution (20 mL) containing salicylic aldehyde (1 mmol, 0.122 g). Then the solution was refluxing for 8 h under stirring and some white precipitate appeared. Excess solvent was removed under reduced pressure. After cooling to room temperature, the mixture was filtered, dried and recrystallized from ethanol. Yield: 53%; mp: 249–250 °C. ^{1}H-NMR (Fig. S3†) (400 MHz; DMSO-d_6): (major): $\delta = 2.74$ (s, $3H_5$), 6.92–6.98 (m, H_{10}, H_{12}), 7.34 (m, H_{11}), 7.54–7.63 (m, H_2, H_9), 7.67 (s, H_6), 7.81(m, H_3), 8.03 (d, $J = 8.3$ Hz, H_4), 8.16 (d, $J = 8.1$ Hz, H_1), 8.57 (s, H_8), 11.03 (s, H_{13}), 12,36 (s, H_7). (Minor): $\delta = 2.71$ (s, $3H_5$), 6.66–6.73 (m, H_{10}, H_{12}), 6.93 (m, H_{11}), 7.04–7.14 (m, H_2, H_9), 7.50 (s, H_6), 7.56 (m, H_3), 7.76 (m, H_4), 8.01 (m, H_1), 8.34 (s, H_8), 9.67 (s, H_{13}), 12, 33 (s, H_7). IR (KBr, cm^{-1}): 3146, 1659, 1562, 1273. ESI-MS (Fig. S4†): $[M + 1]^+$: 306.13. $[M + Na]^+$: 328.11.

3. Results and discussion

3.1. General information

Stock solutions of various cations (1 mM) were prepared using nitrate salts. A stock solution of HL (1 mM) was prepared. The solution of HL was then diluted to 10 μM in ethanol. In titration experiments, for each cation, 2 mL of the HL (10 μM) solution was placed in the quartz optical cell of 1 cm optical path length, and the ion stock solution was gradually added into the quartz optical cell using a pipette. Spectral data were recorded at 3 min after the addition of the ion. In selectivity experiments, the test samples were prepared by placing appropriate amounts of stock ion solution into 2 mL of HL (10 μM) solution. For fluorescence

measurements, the excitation and emission slit widths were 5 nm and 3 nm, respectively.

The binding constant values were determined from the emission intensity data following the modified Benesi–Hildebrand equations.[22–24]

$$\frac{1}{F - F_{\min}} = \frac{1}{K(F_{\max} - F_{\min})[\mathrm{Al}^{3+}]} + \frac{1}{F_{\max} - F_{\min}}$$

where: $F_{\min}$, F, and $F_{\max}$ were the emission intensities of the organic moiety in the absence of aluminum ions, in the presence of an intermediate aluminum concentration, and at a concentration of aluminium where there was complete interaction, respectively, and where K_a is the binding constant concentration.

The detection limit was calculated based on the fluorescence titration. To determine the signal-to-noise ratio,[25,26] the emission intensity of the complex (L–Al) without any anion was 2.5 eq. and the standard deviation of the blank measurements was determined. The detection limit was then calculated with the following equation: detection limit $3\sigma/K$. where σ is the standard deviation of blank measurements, and K is the slope of a curve obtained by plotting intensity *versus* sample concentration.

3.2. UV-Vis analysis

The absorption spectrum of HL exhibits a broad band at 338 nm at room temperature in ethanol. To investigate the binding property of HL towards Al^{3+}, we measured the UV-Vis spectra of HL (25 μM) in the presence of various concentrations of Al^{3+} (Fig. 1). The free receptor in solution shows two absorption bands at 288 nm and 322 nm. Upon the gradual addition of Al^{3+} (0–4.5 eq.) to a solution of HL, the absorption band at 288 nm gradually disappeared, and a new absorption band appears at

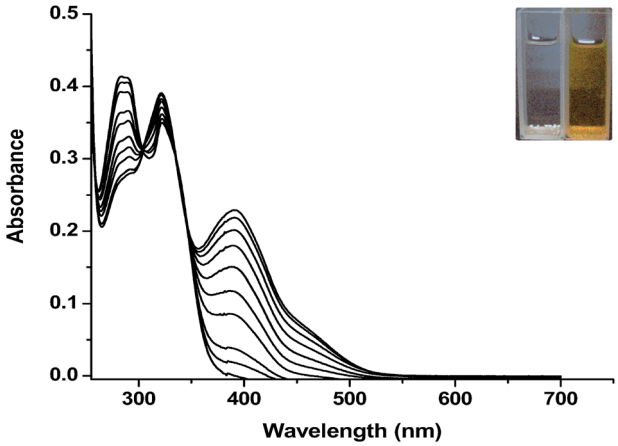

Fig. 1 Changes in the absorption spectra of HL (25 μM) in ethanol at room temperature as a function of added Al^{3+} (0–4.5 eq.). Inset: color of HL and HL + Al^{3+} system under visible light.

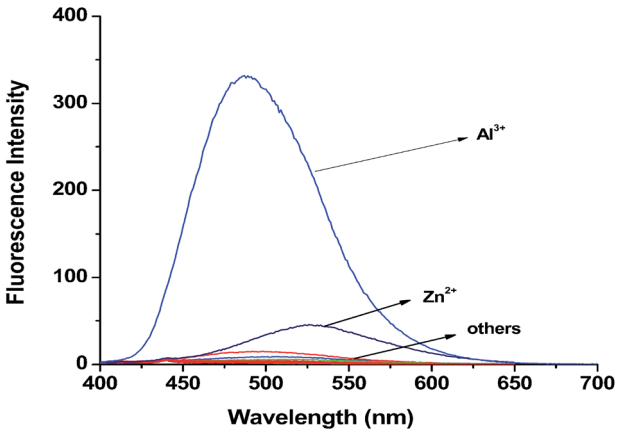

Fig. 2 Fluorescence spectra of HL (10 μM) upon the addition of metal salts (1.0 eq.) of Na^+, K^+, Ca^{2+}, Mg^{2+}, Cu^{2+}, Co^{2+}, Mn^{2+}, Ni^{2+}, Zn^{2+}, Fe^{2+}, Cd^{2+}, Ba^{2+}, Hg^{2+}, Pb^{2+}, Fe^{3+}, Cr^{3+} and Al^{3+} in ethanol. Excitation wavelength was 389 nm.

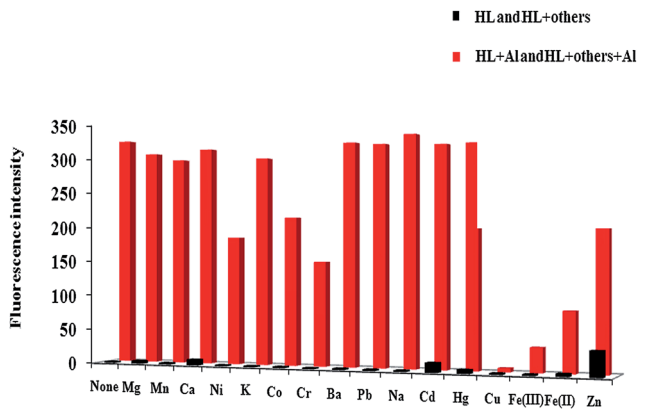

Fig. 3 Fluorescence intensity of HL and its complexation with Al^{3+} in the presence of various metal ions. Black bar: HL (10.0 μM) and HL with 1.0 eq. of Ba^{2+}, Ca^{2+}, Cd^{2+}, Co^{2+}, Cr^{3+}, Cu^{2+}, Fe^{2+}, Fe^{3+}, Hg^{2+}, K^+, Mg^{2+}, Mn^{2+}, Na^+, Ni^{2+}, Pb^{2+}, and Zn^{2+}. Red bar: 10.0 μM of HL and 1.0 eq. of Al^{3+} with 1.0 eq. of metal ions as stated (λ_{ex} = 389 nm).

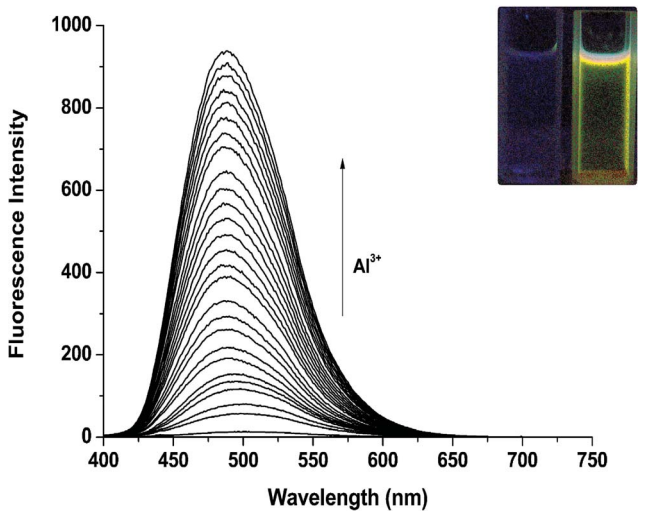

Fig. 4 Fluorescence spectra of HL (10 μM) in ethanol, upon the addition of $Al(NO_3)_3$ (0–25 μM) with an excitation of 389 nm. Inset: color of HL and HL + Al^{3+} system under UV lamp.

389 nm with increasing intensity while two clear isosbestic points at 300 nm, 325 nm, were observed. In addition, a solution of HL was colorless whereas the solution in the presence of Al^{3+} appears yellow under visible light. All of these might contribute to the formation of a 1 : 1 stoichiometry of the binding mode of HL with Al^{3+}, resulting in breaking hydrogen bonds and the deprotonation which was further confirmed by ESI-MS, and ^{1}H-NMR titration.[27]

3.3. Fluorescence study

The free chemosensor HL showed no fluorescence emission at 484 nm when it was excited at 389 nm in ethanol. Upon the addition of 1.0 eq. of Al^{3+}, the chemosensor showed a large fluorescence enhancement (220-fold) at 484 nm. In contrast, addition of other relevant metal ions, such as Ba^{2+}, Ca^{2+}, Cd^{2+}, Co^{2+}, Cr^{3+}, Cu^{2+}, Fe^{2+}, Fe^{3+}, Hg^{2+}, K^+, Mg^{2+}, Mn^{2+}, Na^+, Ni^{2+}, and Pb^{2+} caused almost no fluorescence increase. Zn^{2+} also generated a certain fluorescence enhancement. However, the intensity was significantly lower than with Al^{3+} (Fig. 2). To understand the recognition abilities of HL toward Al^{3+}, competition experiments (Fig. 3) and fluorescent titrations (Fig. 4) were conducted. From the competition experiments, mixing the HL–Al(III) complex with other metal ions showed that no significant variation was observed in fluorescence intensity except in the case of Cu(II), Fe(II), Fe(III). As for Fe^{2+}, Fe^{3+}, and Cu^{2+}, ions the decrease in fluorescence was because these ions typically have a pronounced quenching effect on fluorophores by mechanisms inherent to the paramagnetic species.[28–31] Thus, HL can be used as a selective fluorescent sensor for Al^{3+} relative to most competing metal ions. In the fluorescence titration profile, because of the low coordination ability of Al^{3+} (as a hard-acid), it is extremely difficult to achieve saturation in the titration experiment.[32–35] In order to guarantee the experimental accuracy, a titration experiment carried out using 2.5 eq. of added Al(III) instead of 1.0 eq. From the profile obtained, the binding constant of HL for Al^{3+} has been estimated as 5.6×10^4 based on the modified Benesi–Hildebrand equations. The detection limit for Al^{3+} was calculated to be 7.2×10^{-7} M, which was sufficiently low to allow detection of submicromolar concentrations of Al^{3+}.

3.4. Spectra studies for the complexation of HL with Al^{3+}

From the Job's plot analysis, the results indicated that the binding mode of HL and Al^{3+} showed a 1 : 1 stoichiometry (Fig. 5). To further validate the conjugation of L–Al, ESI-MS, ^{1}H-NMR, and infrared (IR) experiments were carried out. In the ESI-MS spectra (Fig. S5†), a peak at *m*/*z* 348.08 is assigned to $[HL + H_2O + Al^{3+} - 2H]^+$, and a peak at *m*/*z* 376.11 is assigned to $[HL + CH_3CH_2OH + Al^{3+} - 2H]^+$. A doubly charged ion peak at *m*/*z* 165.5 is assigned to $(HL + Al^{3+} - 1)/2$. Thus, this is enough to confirm the formation of a 1 : 1 complex between HL and Al^{3+}.

In ^{1}H-NMR titration, Al^{3+} (as its nitrate salt) was added to the deuterated dimethyl sulfoxide (DMSO-d_6) solution of HL (Fig. S6†). Significant spectral changes were observed (Fig. 6). In the presence of Al^{3+} (1.0 eq.), the free ligand exhibited two imine (–CH=N–) signals at 8.52 and 8.30 ppm, corresponding to the major and minor isomers, respectively. Upon addition of the Al^{3+}cation, a new broad signal was developed at 8.71 ppm, which was attributed to the interaction of the imine-nitrogen and Al^{3+}. In addition, the proton peak of the phenolic hydroxyl at 10.99 ppm and 9.65 ppm disappeared, and the proton signal of the imine downfield shifted by 0.2 ppm. These might be attributed to the binding mode of HL with Al^{3+}, resulting in breaking of hydrogen bonds and deprotonation. From the ^{1}H-NMR spectra it can be seen that new signals at 9.12 ppm appeared. The new signal is because of the active hydrogen signals, which were introduced by hydrated Al(III) salts. This shows that even hydrated Al(III) salts may be sufficient to hydrolyze and form hydrated Al(III) compounds.[36]

In IR spectra (Fig. S7 and S8†), the stretching frequency of the –C=O of the quinoline moiety and Ar–O are decreased by 26 cm^{-1} from 1659 cm^{-1} to 1633 cm^{-1} and by 32 cm^{-1} from 1273 cm^{-1} to 1241 cm^{-1}, respectively. In addition, the vibrational mode of –C=N shifts from 1591 cm^{-1} to 1541 cm^{-1}, reflecting the reduced conjugation effect between –C=N and the aromatic ring. The large differences of the IR spectra of HL in the absence and presence of Al^{3+} indicate that Al^{3+} does directly interact with the nitrogen atom in –C=N and the oxygen atom in –C=O and Ar–O.

3.5. The proposed mechanism

The experiments described previously suggest that HL chelates Al^{3+} through interactions with carboxylate oxygen, imine nitrogen and the oxygen of the phenolic hydroxyl group.[37–40] The sensing mechanism was estimated using the degree of chelation. In solution, the free HL exhibited weak fluorescence because of ESIPT and PET. The interaction between Al^{3+} and HL results in the breaking of the intra-molecular hydrogen bond (OH···N) with the imine-nitrogen and the deprotonation of the phenolic hydroxyl, consequently, inhibiting intramolecular proton transfer in the excited state.[41,42] Another reason is the

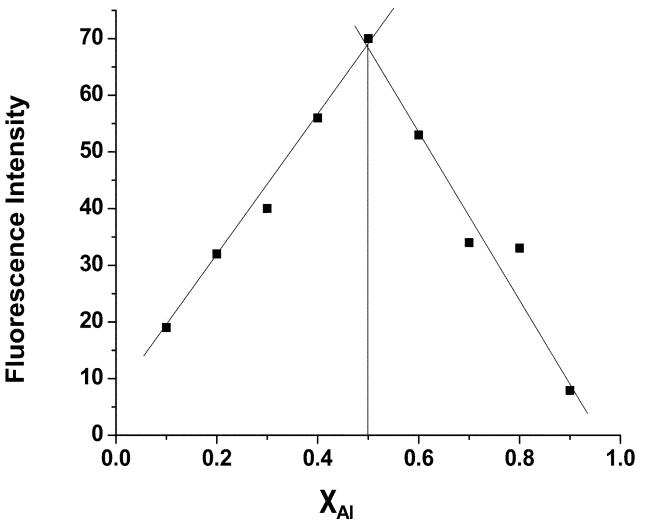

Fig. 5 Job's plot for determining the stoichiometry of HL and Al^{3+} in ethanol ($X_{Al} = [Al^{3+}]/([Al^{3+}] + [HL])$, the total concentration of HL and Al^{3+} was 10 μM).

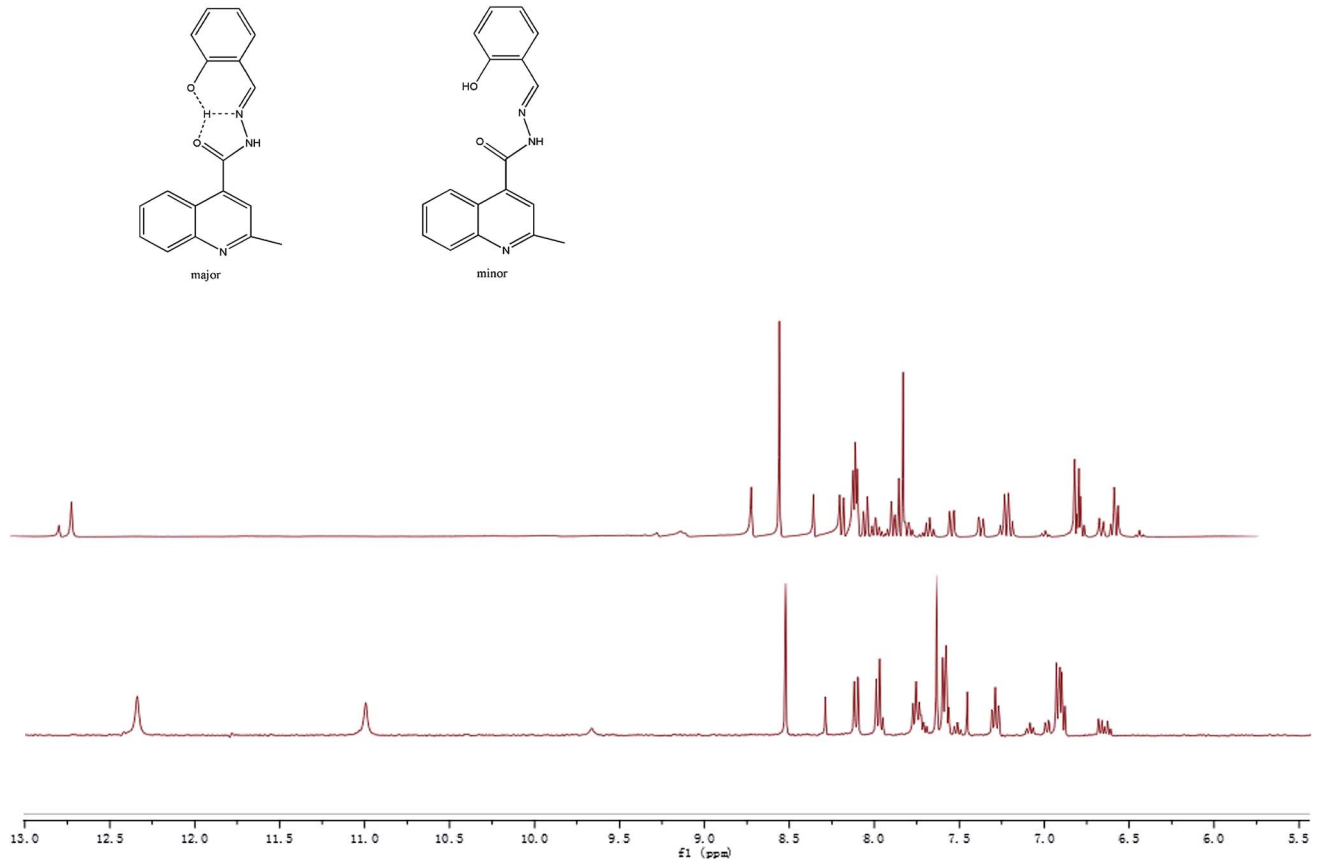

Fig. 6 ^{1}H-NMR spectra of HL with $Al(NO_3)_3 \cdot 9H_2O$ in DMSO-d_6: (I) HL; (II) HL with 1.0 eq. of Al^{3+}; (III) HL with 1.5 eq. of Al^{3+}.

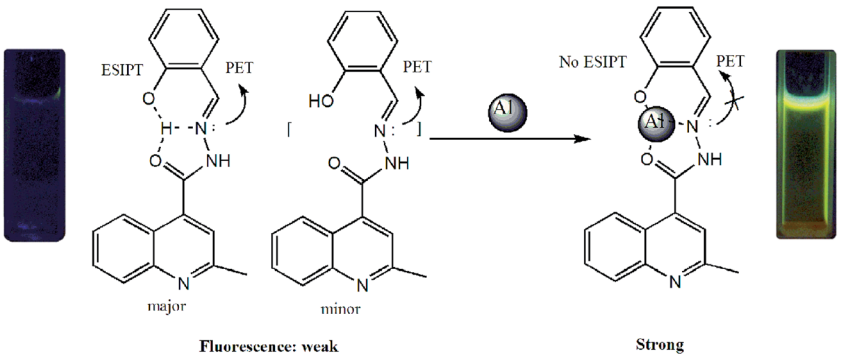

Scheme 2 Proposed mechanism for detection of Al^{3+} by HL.

chelation of the nitrogen atom of the –C=N group with Al^{3+}, which results in efficient inhibition of the –C=N group for the PET process (Scheme 2).[43–47]

4. Conclusion

In summary, we have designed and characterized a chemosensor, which exhibited high selectivity for Al^{3+}. This phenomenon was attributed to the formation of a 1 : 1 stoichiometric complex ($K_a = 5.6 \times 10^4$), which inhibits the photo-induced electron transfer process and the excited-state intramolecular proton transfer process. Upon the addition of Al^{3+}, the chemosensor shows fluorescence enhancement up to 220-fold, and the lowest detection limit for Al^{3+} reaches the 10^{-7} M level, which is lower than many of the other reported Al^{3+} sensors.[48–51] Thus, the probe has sufficient capability to detect the submicromolar concentration of the Al^{3+} in the environment. Meanwhile, we will now be actively studying its application in physiological conditions.

Acknowledgements

This work is supported by the National Natural Science Foundation of China (81171337).

References

1 V. K. Gupta, A. K. Jain and G. Maheshwari, *Talanta*, 2007, **72**, 1469.
2 T. P. Flaten, *Brain Res. Bull.*, 2001, **55**, 187–196.
3 J. Tria, E. C. V. Butler, P. R. Haddad and A. R. Bowie, *Anal. Chim. Acta*, 2007, **588**, 153.
4 L. H. Zhi, J. Liu, Y. Wang, W. Zhang, B. D. Wang, Z. G. Xu, Z. Y. Yang, X. Huo and G. G. Li, *Nanoscale*, 2013, **5**, 1552.
5 Z. Krejpcio and R. W. Wojciak, *Pol. J. Environ. Stud.*, 2002, **11**, 251.
6 K. Soroka, R. S. Vithanage, D. A. Phillips, B. Walker and P. K. Dasgupta, *Anal. Chem.*, 1987, **59**, 627.
7 S. Kim, J. Y. Noh, K. Y. Kim, J. H. Kim, H. K. Kang, S. W. Nam, S. H. Kim, S. Park, C. Kim and J. Kim, *Inorg. Chem.*, 2012, **51**, 3597.
8 W. Gruber and J. Herbauts, *Analysis*, 1990, **118**, 12.
9 J. Quinonero, C. Mongay and M. D. Guardia, *Microchem. J.*, 1991, **43**, 213.
10 Q. T. Cai and S. B. Khoo, *Anal. Chim. Acta*, 1993, **276**, 99.
11 Y. K. Jang, U. C. Nam, H. L. Kwon, I. H. Hwang and C. Kim, *Dyes Pigm.*, 2013, **99**, 6.
12 H. M. Park, B. N. Oh, J. H. Kim, W. Qiong, I. H. Hwang, K. D. Jung, C. Kim and J. Kim, *Tetrahedron Lett.*, 2011, **52**, 5581.
13 J. L. Ren, J. Zhang, J. Q. Luo, X. K. Pei and Z. X. Jiang, *Analyst*, 2001, **126**, 698.
14 Y. W. Wang, M. X. Yu, Y. H. Yu, Z. P. Bai, Z. Shen, F. Y. Li and X. Z. You, *Tetrahedron Lett.*, 2009, **50**, 6169.
15 S. H. Kim, H. S. Choi, J. Kim, S. J. Lee, D. T. Quang and J. S. Kim, *Org. Lett.*, 2010, **12**, 560.
16 Y. Zhao, Z. Lin, H. Liao, C. Duan and Q. Meng, *Inorg. Chem. Commun.*, 2006, **9**, 966.
17 K. K. Upadhyay and A. Kumar, *Org. Biomol. Chem.*, 2010, **8**, 4892.
18 X. Sun, Y. W. Wang and Y. Peng, *Org. Lett.*, 2012, **14**, 3420.
19 J. S. Zugazagoitia, M. Maya, C. D. Zea, P. NavarroBeltrá and H. I. Peon, *J. Phys. Chem. A*, 2010, **114**, 704.
20 S. Guha, S. Lohar, A. Sahana, A. Banerjee, D. A. Safin, M. G. Babashkina, M. P. Mitoraj, M. Bolte, Y. Garcia, S. K. Mukhopadhyaye and D. Das, *Dalton Trans.*, 2013, **42**, 10198.
21 J. Deng, N. Li, H. C. Liu, Z. L. Zuo, O. W. Liew, W. J. Xu, G. Chen, X. K. Tong, W. Tang, J. Zhu, J. P. Zuo, H. L. Jiang, C. G. Yang, J. Li and W. L. Zhu, *J. Med. Chem.*, 2012, **55**, 6278.
22 Y. K. Jang, U. C. Nama, H. L. Kwon, I. H. Hwang and C. Kim, *Dyes Pigm.*, 2013, **99**, 6.
23 T. J. Jia, W. Cao, X. J. Zheng and L. P. Jin, *Tetrahedron Lett.*, 2013, **54**, 3471.
24 T. Sen, B. Mukherjee, A. Chattopadhyay, A. M. Basu, J. Marekd and P. Chattopadhyay, *Analyst*, 2012, **137**, 3975.
25 L. Long and J. D. Winefordner, *Anal. Chem.*, 1983, **55**, 712A.
26 J. M. Kim, S. Y. Chung, J. Y. Yoon and K. H. Lee, *Analyst*, 2010, **135**, 2079.
27 V. P. Singh, K. P. iwari, M. shra, N. Srivastava and S. Saha, *Sens. Actuators, B*, 2013, **182**, 546.
28 J. M. An, M. H. Yan, Z. Y. Yang, T. R. Li and Q. X. Zhou, *Dyes Pigm.*, 2013, **99**, 1.
29 T. T. Zhang, X. P. Chen, J. T. Liu, L. Z. Zhang, J. M. Chu, L. Su and B. X. Zhao, *RSC Adv.*, 2014, **4**, 16973.
30 D. Maity and T. Govindaraju, *Inorg. Chem.*, 2010, **49**, 7229.
31 C. J. Gao, X. Liu, X. J. Jin, J. Wu, Y. J. Xie, W. S. Liu, X. J. Yao and Y. Tang, *Sens. Actuators, B*, 2013, **185**, 125.
32 H. Liu, X. Hao, C. H. Duan, H. Yang, Y. Lv, H. J. Xu, H. D. Wang, F. Huang, D. B. Xiao and Z. Y. Tian, *Nanoscale.*, 2013, **5**, 9340.
33 X. J. Xie and Y. Qin, *Sens. Actuators, B*, 2011, **156**, 213.
34 S. Samanta, B. Nath and J. B. Baruah, *Inorg. Chem. Commun.*, 2012, **22**, 98.
35 Z. Q. Li, Q. P. Hu, C. X. Li, J. T. Dou, J. J. Cao, W. K. Chen and Q. Z. Zhu, *Tetrahedron Lett.*, 2014, **55**, 1258.
36 W. H. Ding, W. Cao, X. J. Zheng, W. J.Ding, J. P. Qiao and L. P. Jin, *Dalton Trans.*, 2014, **43**, 6429.
37 V. P. Singh, K. Tiwari, M. Mishra, N. Srivastava and S. Saha, *Sens. Actuators, B*, 2013, **182**, 546.
38 D. Karak, S. Lohar, A. Banerjee, A. Sahana, I. Hauli, S. K. Mukhopadhyay, J. S. Matalobos and D. Das, *RSC Adv.*, 2012, **2**, 12447.
39 D. Karak, S. Lohar, A. Sahana, S. Guha, A. Banerjee and D. Das, *Anal. Methods*, 2012, **4**, 1906.
40 W. H. Hsieh, C. F. Wan, D. J. Liao and A. T. Wu, *Tetrahedron Lett.*, 2012, **53**, 5848.
41 Y. P. Li, Q. Zhao, H. R. Yang, S. J. Liu, X. M. Liu, Y. H. Zhang, T. L. Hu, J. T. Chen, Z. Chang and X. H. Bu, *Analyst*, 2013, **138**, 5486.
42 J. F. Wang and Y. Pang, *RSC Adv.*, 2014, **4**, 5845.
43 Z. C. Liao, Z. Y. Yang, Y. Li, B. D. Wang and Q. X. Zhou, *Dyes Pigm.*, 2013, **97**, 119.
44 L. Fan, T. R. Li, B. D. Wang, Z. Y. Yang and C. J. Liu, *Spectrochim. Acta, Part A*, 2014, **118**, 760.
45 P. Alaei, S. Rouhani, K. Gharanjiga and J. Ghasemi, *Spectrochim. Acta, Part A*, 2012, **90**, 85.
46 T. Gunnlaugsson, A. P. Davis, J. E. O'Brien and M. Glynn, *Org. Lett.*, 2002, **4**, 2449.
47 M. M. Yu, R. L. Yuan, C. X. Shi, W. Zhou, L. H. Wei and Z. X. Li, *Dyes Pigm.*, 2013, **99**, 887.
48 A. Sahana, A. Banerjee, S. Das, S. Lohar, D. Karak, B. Sarkar, S. K. Mukhopadhyay, A. K. Mukherjee and D. Das, *Org. Biomol. Chem.*, 2011, **9**, 5523.
49 D. Maity and T. Govindaraju, *Chem. Commun.*, 2012, **48**, 1039.
50 C. H. Chen, D. J. Liao, C. F. Wan and A. T. Wu, *Analyst*, 2013, **138**, 2527.
51 R. X. Kang, X. M. Shao, F. F. Peng, Y. L. Zhang, G. T. Sun, W. L. Zhao and X. D. Jiang, *RSC Adv.*, 2013, **3**, 21033.

